

Electron scattering in ethene: Excitation of the \tilde{a}^3B_{1u} state, elastic scattering, and vibrational excitation

M. Allan

Department of Chemistry, University of Fribourg, Chemin du Musée 9, CH-1700 Fribourg, Switzerland

C. Winstead and V. McKoy

A. A. Noyes Laboratory of Chemical Physics, California Institute of Technology, Pasadena, California 91125, USA

(Received 8 February 2008; published 16 April 2008)

Experimental and calculated absolute differential cross sections for the scattering of low-energy electrons from ethene are presented. Emphasis is on the excitation of the $\tilde{a}^3B_{1u}^3(\pi, \pi^*)$ state, but selected elastic and vibrational excitation cross sections are also given. In contrast to earlier calculations, which were nearly a factor of 2 too large, the present calculation agrees very well with the experimental triplet excitation cross section in the threshold region. The improvement is due primarily to the inclusion of target polarization, which results in proper positioning of the π^* resonance, whose high-energy tail dominates the triplet state excitation near threshold. The present experimental elastic cross sections agree very well with recent calculations taking into account target polarization.

DOI: [10.1103/PhysRevA.77.042715](https://doi.org/10.1103/PhysRevA.77.042715)

PACS number(s): 34.80.Gs, 34.80.Bm

I. INTRODUCTION

Ethene is the prototype of unsaturated hydrocarbons and as such an important molecule for testing various theoretical methods. It is a particularly suitable model for electronic excitation—the $^3(\pi, \pi^*) \tilde{a}^3B_{1u}$ lowest electronically excited state is energetically well separated from higher excitations. This status motivated numerous experimental and theoretical studies.

Sueoka and Mori [1] reported experimental grand total cross sections for electrons and positrons in the range 0.7–400 eV. Mapstone and Newell [2] measured the elastic cross section from 3.3 to 15.5 eV in the 30°–140° angular range. Lunt *et al.* [3] measured the elastic and vibrational excitation cross sections in the threshold region below 2 eV using synchrotron electron sources. Panajotović *et al.* [4] presented an extensive experimental study of the elastic cross sections and a cross section for exciting the C–H stretch vibrations at 7.5 eV. Khakoo *et al.* recently measured the elastic cross section, avoiding the problem of varying gas beam profile by using an aperture instead of a capillary to introduce the sample [5].

These experiments can be compared to several calculations of the elastic cross sections. Winstead *et al.* [6] reported static-exchange elastic cross sections. Polarization was included in the more recent study of Winstead *et al.* [7]. Schneider *et al.* [8] performed a complex Kohn calculation of the total cross section and found a Ramsauer-Townsend minimum. Trevisan *et al.* [9] reported calculations of the elastic cross section which describe the dynamic polarization of the target by the incident electron and involve calculations over a range of different geometries, including the effects of nuclear motion in the resonant $^2B_{2g}$ symmetry with an adiabatic nuclei treatment of the C–C stretch mode.

There are only few calculations of electronic excitation. Sun *et al.* [10] reported a two-state close coupling calculation of differential and integral cross sections for the excitation of the $\tilde{a}^3B_{1u}(\pi, \pi^*)$ state using the Schwinger multi-channel method. Rescigno and Schneider [11] reported the

differential and the integral cross sections for the excitation of both the triplet and the singlet (π, π^*) states. They found a significant *d*-wave resonant behavior in the triplet cross section near 5 eV. Recent calculations by da Costa *et al.* [12] explored the effect of polarization on the cross section for excitation of the triplet (π, π^*) state.

The relative integral cross section for excitation of the $^3(\pi, \pi^*)$ state in ethene by electron impact was measured by Van Veen [13] using the trapped electron method. Relative measurements of the differential cross section at 0°, measured with a magnetically collimated spectrometer, were reported by Love and Jordan [14]. The absolute differential cross sections for the excitation of the $^3(\pi, \pi^*)$ state were measured in this laboratory previously [15]. The angular range was extended to 180° using a combination of a spectrometer with hemispherical energy analyzers and a magnetically collimated spectrometer with pulsed electron beam and electron time-of-flight detection, capable of measuring the ratio of 0° and 180° cross sections [16]. The results of these measurements were about a factor of 2 lower than all theoretical predictions. This standing problem was recently pointed out by da Costa *et al.* [12], who also noted the important role of polarization, required to properly place the shape resonances. However, the exploratory calculations of da Costa *et al.* did not bring the calculated cross section into better agreement with experiment.

It thus appears important to test the possibility that the discrepancy is due to an error of the measurement, and likewise to test whether a fuller description of polarization might affect the calculated results. This paper is primarily devoted to these tests: the measurement of the electronic excitation cross sections makes use of improved techniques for calibrating the response functions of the spectrometer [17], and of the advent of the magnetic angle changer [18], while the calculation employs a systematic and extensive treatment of polarization. Selected measurements of the elastic and vibrational excitation cross sections are also presented, with the main goal of extending existing data to larger scattering angles.

II. METHODS

A. Experiment

The measurements were performed using a spectrometer with hemispherical analyzers [17,19,20]. The energy resolution was about 20 meV in the energy-loss mode, corresponding to about 15 meV in the incident electron beam, at a beam current of around 400 pA. The energy of the incident beam was calibrated on the 19.365 eV [21] 2S resonance in helium and is accurate to within ± 10 meV. The instrumental response function was determined on elastic scattering in helium and all spectra were corrected as described earlier [17]. Absolute values of the cross sections were determined by the relative flow technique as described by Nickel *et al.* [22] using the theoretical helium elastic cross sections of Nesbet [23] as a reference. The confidence limit is about $\pm 20\%$ for the elastic cross sections and $\pm 25\%$ for the electronically inelastic cross sections (two standard deviations). The ethene and helium pressures in the gas inlet line were typically 0.08 and 0.23 mbars, respectively, during the absolute measurements. Background was determined by recording signal with gas flowing into the main chamber via a bypass line and not the nozzle. This background was generally negligible except in the more forward scattering and at low energies, but for consistency the “bypass signal” was subtracted even when it was very low.

The angular distributions were measured using combined mechanical setting of the analyzer and magnetic deflection by the magnetic angle changer [18,24], correcting the curves for the instrumental response function, and fitting them to the discrete absolute values measured at 45°, 90°, 135°, and 180°, as described in Ref. [17]. The angle was incremented in steps of 5°.

B. Theory

Electron-impact excitation cross sections for the \tilde{a}^3B_{1u} state were computed using the Schwinger multichannel method [25] as implemented for parallel computers [26,27]. The calculation employed the same molecular geometry and one-electron basis set as was used in a recent calculation on elastic scattering [7] and followed, insofar as possible, the same procedure for constructing a variational space of many-electron functions, the only differences being that all doublets that could be built from the \tilde{a}^3B_{1u} state were included as open-channel configurations, and that the lowest b_{2g} modified virtual orbital (MVO) [28] was replaced with the appropriate $^3(\pi, \pi^*)$ improved virtual orbital [29], to which the remaining b_{2g} MVOs were then orthogonalized. The configurations built on singlet-coupled single excitations of the target that were included to represent polarization were treated as belonging to the closed-channel space at all energies. As the energy increases and additional excitation and ionization channels open, this becomes an increasingly poor approximation, and the calculated cross sections accordingly grow unreliable. However, up to the $(\pi, \pi^*)^1B_{1u}$ threshold, ~ 8 eV, including only two open electronic channels is the correct description, and good results may thus be anticipated in this near-threshold region.

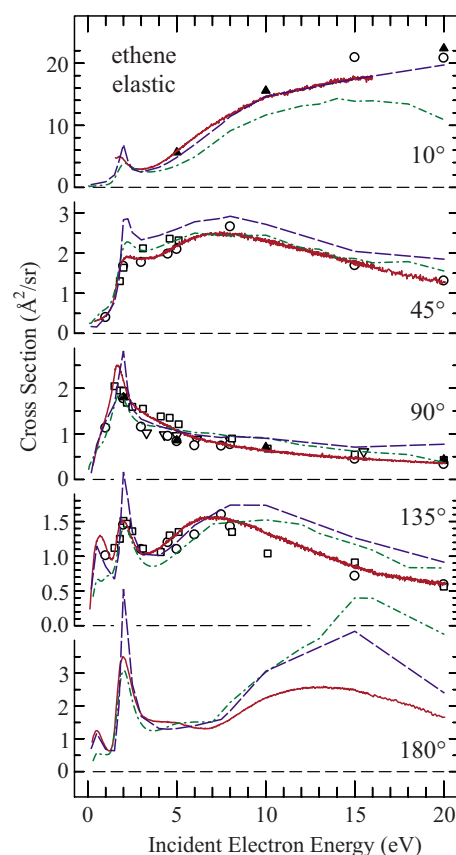


FIG. 1. (Color online) Elastic cross sections shown as a function of electron energy. Continuous lines show the results of the present experiment, dashed lines the calculations of Winstead *et al.* [7], and dash-dotted lines the calculations of Trevisan *et al.* [9]. Also shown are the experimental data of Khakoo *et al.* [5] (\blacktriangle), of Mapstone and Newell [2] (∇), and the ANU (\circ) and the Sophia (\square) data of Panajotović *et al.* [4]. The average of the 40° and 50° ANU and Sophia data is shown in cases where 45° data were not available. The 130° ANU and Sophia data are compared to the present 135° cross sections.

III. RESULTS AND DISCUSSION

A. Elastic scattering

Absolute elastic cross sections were measured at 1.5, 3, 6, 10, 15, and 20 eV, at each of the scattering angles of 45°, 90°, 135°, and 180°. An excitation function was then measured at $\Delta E = 0$ eV at each of these angles (and also at 10°) and normalized to the absolute values obtained in the previous step. (The absolute value at 10° was not measured explicitly, but derived from the angular distribution measurement described below.) The results are shown in Fig. 1. The data at 10° and 180° were recorded with the aid of the magnetic angle changer.

The present absolute values agree well with the earlier experimental results of Refs. [2,4,5]. The present elastic cross sections below 1 eV at 90° compare favorably also with the low-energy measurement of Lunt *et al.* [3] (which extend down to 0.08 eV), in terms of both shape and magnitude.

Very satisfactory agreement is found with the cross sections calculated by Winstead *et al.* [7]. In particular, the

agreement is very good down to low energies, at all scattering angles, even below the ${}^2B_{2g} \pi^*$ shape resonance which is manifested as a peak around 1.8–2 eV in all spectra. (The exact position of the peak depends on scattering angle.) The agreement confirms that polarization effects, decisive at low energies, were treated correctly in this calculation. This is also reflected in the fact that the resonance is calculated only very slightly above the experimental energy; calculations neglecting polarization tend to overestimate the resonance energies by several eV. The height of the resonance peak is overestimated in the calculation, presumably because the fixed-nuclei calculation makes the resonance too sharp and fails to distinguish vibrationally elastic and vibrationally inelastic channels [7]. An excellent degree of agreement is also seen with the calculated cross sections of Trevisan *et al.* [9]. This calculation incorporates an adiabatic-nuclei treatment of symmetric stretch motion which lowers the height of the 1.8 eV resonant peak and improves the agreement with experiment in the resonant region.

The present measurements become substantially less precise below about 0.1 eV, but evidence for a Ramsauer-Townsend minimum at 0.08 eV was found in the 135° cross section, in qualitative agreement with the theoretical work of Schneider *et al.* [8], who predicted a minimum at 0.2 eV, and later by Winstead *et al.* [7], who predicted a minimum at 0.15 eV. Both predictions were made in the A_g symmetry component of the integral cross section. This minimum appears to be partially washed out when all symmetry components are included in the calculation [7]. A Ramsauer-Townsend minimum was proposed, based on previous electron transport experiments, by Hayashi [30] in the momentum-transfer cross section at 0.08 eV.

A second minimum appears at 1.21 eV in the 180° and 135° spectra, similar to those observed at large scattering angles in many molecules [31]. It is well reproduced by theory. The calculations overestimate the cross section in the 9–20 eV range at 135° and 180° .

The angular distributions of the elastic signal (measuring not the heights of the elastic peaks, but the integral under them) were then measured at 1.5 and 5 eV and normalized to the absolute values. The data were recorded in three overlapping intervals (0° – 90° , 45° – 135° , 90° – 180°) which were joined together as in the earlier work [17]. The absolute elastic cross sections at 5 eV were taken from the curves in Fig. 1. The results are shown in Fig. 2, and the corresponding integral and momentum-transfer cross sections in Table I. The cross section at 1.5 eV is reminiscent of a d_π wave, confirming that it is strongly affected by the ${}^2B_{2g}(\pi^*)$ shape resonance. The agreement with earlier data is satisfactory, except below 60° at 1.5 eV, where the present data rise, but some of the earlier data stay approximately constant or even slightly decrease with decreasing angle. The data recorded by Khakoo *et al.* [5] at an energy 0.5 eV higher, at 2 eV, are consistent with the present measurements: they also rise with decreasing angle below about 40° .

The comparison with the calculated data of Winstead *et al.* [7] is complicated by the somewhat unfortunate choice of the energy: 1.5 eV is on the low-energy tail of the π^* resonance. This has the consequence that the experimental cross section is still strongly affected by the resonance, because of

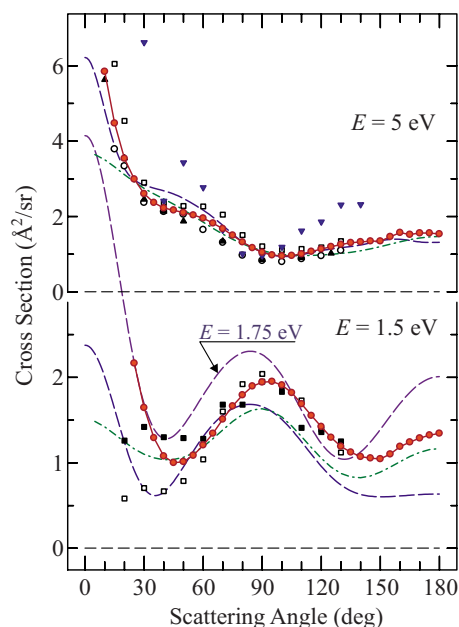


FIG. 2. (Color online) Elastic cross sections shown as a function of scattering angle. Circles connected by a line show the present data, dashed lines the calculations of Winstead *et al.* [7], and dash-dotted lines the calculations of Trevisan *et al.* [9]. The experimental data of Khakoo *et al.* [5] (\blacktriangle), the ANU (\circ) and the Sophia (\square) data of Panajotović *et al.* [4], and the data of Mapstone and Newell [2] (\blacktriangledown) are also shown. Filled squares (\blacksquare) show the Sophia data at 1.8 eV.

its Franck-Condon width, whereas it is below the resonance in the fixed-nuclei calculation. This becomes evident when regarding the calculated cross section at 1.75 eV, also shown in Fig. 2. The two calculated cross sections at energies only 0.25 eV apart differ quite dramatically. The shape of the experimental cross section ($>130^\circ$) is approximately in between that of the calculated cross sections at 1.5 and 1.75 eV: it rises with increasing angle, more than the calculated result at 1.5 eV but less than that at 1.75 eV. The experimental cross section also agrees well with the 1.75 eV calculated cross section around 30° , both rising steeply with decreasing angle. These points of agreement strongly suggest that the calculation of Winstead *et al.* [7] describes correctly the electronic part of the problem and that very good agreement would be obtained if the Franck-Condon width of the π^* resonance were taken into account. The Franck-Condon width is substantial because the temporary occupation of the antibonding π^* orbital lengthens the C=C bond. There is a small difference in that the experimental cross section peaks at 95° and the theoretical cross sections at 85° . The present shape is also in good agreement with the calculations of Trevisan *et al.* at 1.8 eV [9], which include the effects of nuclear motion in the resonant ${}^2B_{2g}$ symmetry with an adiabatic nuclei treatment of the C=C stretch mode.

The angular distributions in Fig. 2 were visually extrapolated to 0° and integrated to yield the integral and momentum-transfer cross sections listed in Table I. The present data agree within error limits with the measurements of Ref. [4]. At 5 (5.1) eV the present data are close to the average of the ANU and the Sophia data of Ref. [4]. The

TABLE I. Integral (ICS) and momentum-transfer (MTCS) elastic cross sections (\AA^2). The error bar of the present data is $\pm 20\%$, that of Ref. [4] 20%–25%, and that of Ref. [1] $\pm 1.4 \text{\AA}^2$ and $\pm 1.1 \text{\AA}^2$ at 1.5 and 5 eV, respectively.

Energy (eV)	ICS			Total CS		MTCS	
	Present	Ref. [4]	Ref. [7]	Ref. [1]	Present	Ref. [4]	Ref. [7]
1.5	19.3	16.3 ^a	14.6	21.9	18.2	16.8 ^a	13.6
5	20.2	17.0 ^b	20.7	22.1	16.4	13.3 ^b	16.3
5.1		22.9 ^a				18.5 ^a	

^aSophia data.

^bANU data.

present energy-loss spectra recorded at several scattering angles indicate that the cross section for the excitation of all vibrations together (including all overtones and combination vibrations) is about 10%–15% of the elastic cross section, at both 1.5 and 5 eV. The present data are thus in very good agreement with the grand total cross sections of Sueoka and Mori [1], which are 14% and 9% higher than the present elastic data at 1.5 and 5 eV, respectively.

B. Excitation of the \tilde{a}^3B_{1u} triplet state

Cross sections for triplet excitation were obtained by recording energy-loss spectra at the discrete incident energies of 6, 10, 15, and 20 eV, correcting them for the instrumental response function, evaluating the areas under the elastic peak and the triplet band, and then normalizing to the absolute elastic cross sections described in the previous section. The excitation functions in Fig. 3 were measured at the energy loss of $\Delta E = 4.2$ eV, but were normalized to express the differential cross section (DCS) integrated over the entire Franck-Condon width of the triplet band ($\Delta E = 3.2$ – 5.9 eV).

The present results are somewhat higher than the previous [16] values, but the two measurements are within the $\pm 35\%$ confidence limit given in Ref. [16]. The present and the previous curves agree well in shape. This is particularly encouraging because the 0° and 180° curves in Ref. [16] were obtained with a different technique, using a magnetically collimated spectrometer with a reflector for electrons scattered into 180° , and with electron time-of-flight resolution. The shape of the present cross section at 0° agrees well with the relative measurement using a magnetically collimated spectrometer of Love and Jordan [14]. The peak around 7 eV in the cross sections was assigned to a $^2(\pi, \pi^{*2})$ core-excited resonance [14–16].

The calculations of Sun *et al.* [10] reproduce the main qualitative features of the experimental shapes: the cross section at 90° consists of a shoulder above threshold and a broad resonant peak, which is at 7 eV in the experiment and about 8.5 eV (at 90°) in the calculation. Such a shift of resonances to higher energy is commonly found with calculations that do not take polarization into account. The resonance shifts to higher energies with increasing angle. The cross section at 180° has a broad hump in the about 8–14 eV range. The calculated cross sections of Sun *et al.* are about 60% larger than the experimental values, however.

In contrast, the present calculations yield cross sections that are similar in shape to the earlier results but agree much better in magnitude with the experimental data. Agreement is particularly good in the immediate threshold region, while the peak in the cross section continues to be placed somewhat too high in energy. Above about 8 eV, the calculated results become larger than the experimental values and begin to exhibit sharp structure due to pseudoresonances. Both features may be attributed to the calculation treating as closed electronic channels that are in fact open. The quality of the calculation continues to deteriorate with increasing energy, and accordingly results are shown only up to 10 eV.

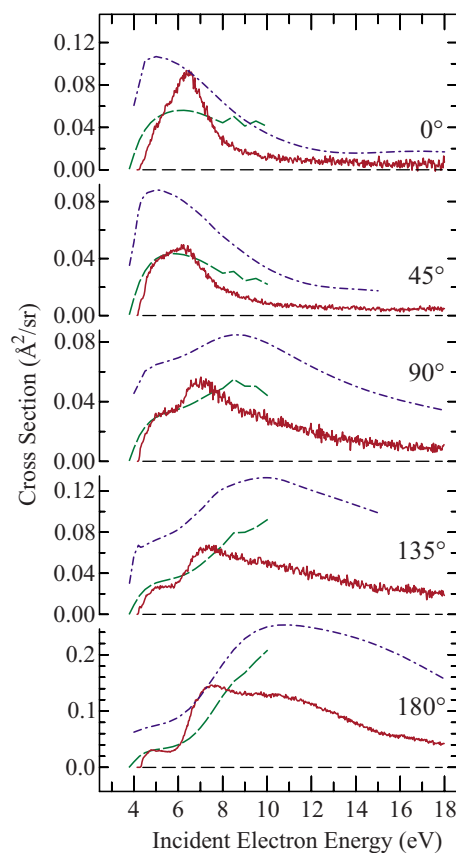


FIG. 3. (Color online) Cross sections for exciting the \tilde{a}^3B_{1u} triplet state, summed over all rovibrational transitions. Dash-dotted lines show the calculated results of Sun *et al.* [10], dashed lines the present theoretical data.

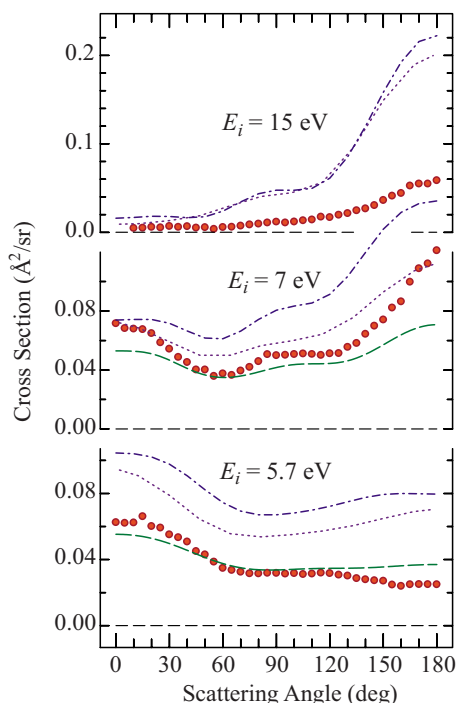


FIG. 4. (Color online) DCS for the excitation of the \tilde{a}^3B_{1u} state shown as a function of scattering angle. Dash-dotted lines show the calculated results of Sun *et al.* [10] (at 5.5, 7.5, and 14.5 eV), dashed lines the present theoretical data (at 5.75 and 7 eV), and dotted lines the calculation of Rescigno and Schneider [11] (at 6, 7, and 15 eV).

The elastic peaks (and vibrational energy loss spectra—see the next section) and the triplet energy-loss bands were then measured in 5° intervals in the three overlapping angular intervals as above and connected together to give the curves shown in Fig. 4. Corresponding integral and momentum-transfer cross sections are given in Table II. The shapes of the angular distributions are compatible with those measured ten years ago, including the $180^\circ:0^\circ$ ratios, although a very different technique was used to obtain them. The principal features of the shapes of the curves agree well with the available calculated results—the cross section at 5.7 eV, below the core-excited resonance, is slightly forward peaked, the cross section at 7 eV, at the core-excited resonance, is slightly backward peaked and reminiscent of a d wave, with a maximum around 90° , and the cross section at 15 eV, above the core-excited resonance, is strongly backward peaked. The larger experimental values of this work

TABLE II. \tilde{a}^3B_{1u} integral and momentum-transfer cross sections (\AA^2).

Energy (eV)	Experiment		Calculation	
	ICS	MTCS	ICS	MTCS
5.7	0.444	0.388	0.470 ^a	0.443 ^a
7.0	0.655	0.713	0.552	0.583
15.0	0.181	0.249		

^aAt 5.75 eV.

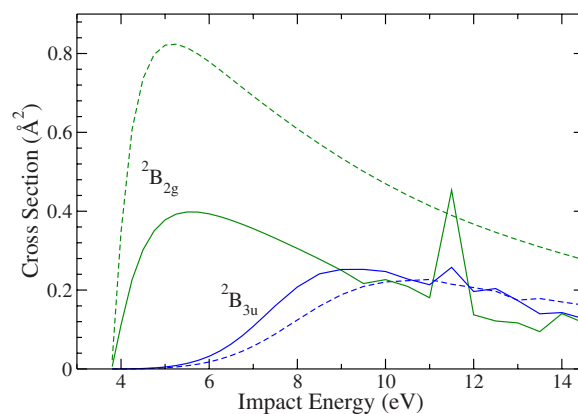


FIG. 5. (Color online) Contributions to the \tilde{a}^3B_{1u} excitation cross section from $^2B_{2g}$ and $^2B_{3u}$ symmetries, calculated with (solid lines) and without (dashed lines) inclusion of polarization effects.

compared to the earlier work improve the agreement with earlier calculations in terms of absolute magnitudes, but the calculated values are still larger, particularly at 15 eV. However, the discrepancy at 5.7 and at 7 eV is removed by the present calculation.

Two of the three main symmetry contributions to the calculated integral cross section for \tilde{a}^3B_{1u} excitation are shown in Fig. 5. For comparison, the same contributions obtained without polarization effects (by deleting all closed-channel configurations from the variational space) are also shown. The sharp rise at threshold is seen to be due to the $^2B_{2g}$ contribution. As pointed out by Rescigno and Schneider [11], $^2B_{2g}$ is the symmetry of the π^* shape resonance in the elastic channel, and the threshold rise may thus be attributed to the high-energy tail of that resonance decaying into the triplet excitation channel. Inclusion of polarization dramatically decreases the magnitude of this contribution to the excitation cross section, consistent with the resonance shifting lower in energy and the triplet threshold thus falling farther out in its tail. Overestimation of the $^2B_{2g}$ contribution in earlier calculations that omitted polarization [10,11] appears to account for the discrepancy between those calculations and experiment.

The second major contribution to the excitation cross section comes from $^2B_{3u}$ symmetry and peaks several eV above threshold. Inclusion of polarization has only a small effect on the magnitude of this contribution but shifts the location of the peak lower by about 2 eV, to near 9 eV. Although somewhat too high in energy, this feature is of the correct symmetry to support the previous assignment of the experimental peak near 7 eV to a (π, π^{*2}) core-excited shape resonance [14–16]. The third main contribution to the triplet cross section, not shown in the figure, comes from $^2B_{1u}$ and rises monotonically from threshold until the onset of pseudoresonances above 10 eV.

C. Vibrational excitation

The selected vibrational excitation cross sections shown in Fig. 6 are compatible in shape with those measured at 90° by Walker *et al.* [32]—they are dominated by the $^2B_{2g} \pi^*$

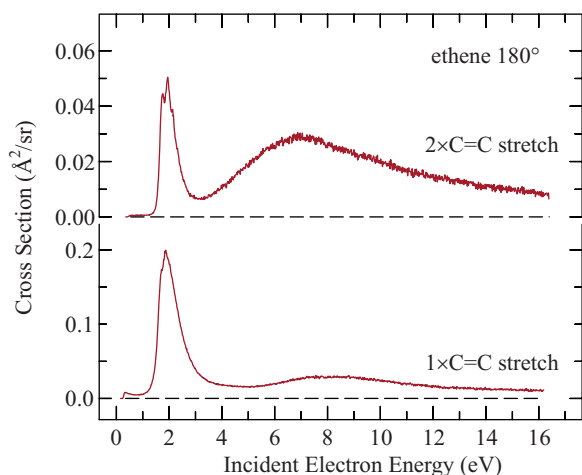


FIG. 6. (Color online) DCS for the excitation of one and two quanta of the C=C stretch vibration ν_2 .

resonance discussed above in connection with the elastic cross section and with near threshold electronic excitation, and known already from the early transmission work of Burrow and Jordan [33]. The broad band peaking around 7.5 eV was assigned as a ${}^2A_g \sigma^*$ resonance by Walker *et al.* [32].

Figure 7 shows the known [32] boomerang structure of the ${}^2B_{2g} \pi^*$ resonance in more detail. The structure becomes deeper for higher overtones, as already observed by Walker *et al.* [32], and similarly to other molecules, for example N_2 and CO [34].

Finally, Fig. 8 shows two representative angular distributions for the excitation of the C=C stretch vibration in the ${}^2B_{2g} \pi^*$ resonance region. The shape of the curves is strongly reminiscent of a d_π wave, consistent with excitation

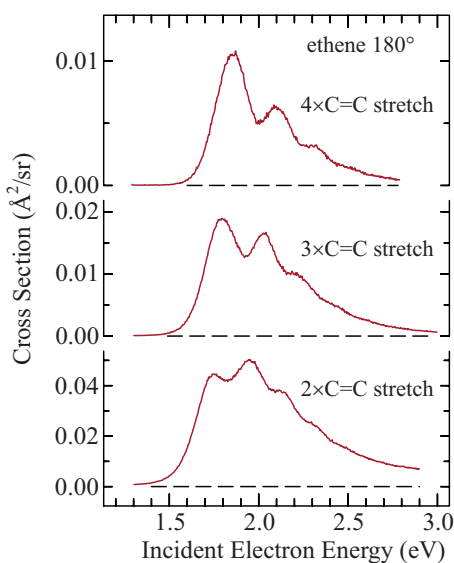


FIG. 7. (Color online) DCS for the excitation of two, three and four quanta of the C=C stretch vibration ν_2 in the range of the π^* resonance.

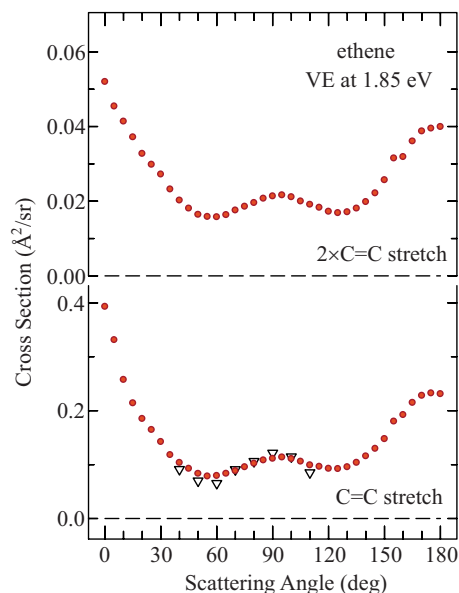


FIG. 8. (Color online) DCS for the excitation of one and two quanta of the C=C stretch vibration ν_2 ($\Delta E=0.201$ and 0.400 eV, resp.), shown as a function of scattering angle. Inverted empty triangles (∇) indicate the data of Walker *et al.* [32].

via the ${}^2B_{2g} (\pi^*)$ shape resonance. The absolute values agree well with the earlier results of Walker *et al.* [32].

IV. CONCLUSIONS

The present cross sections for the excitation of the triplet (π, π^*) state are slightly higher than those of Ref. [16], the difference being probably due to an imperfect determination of the instrumental response function in the earlier work. But even the new measurements are substantially lower than those obtained by previous *ab initio* theories. This discrepancy is removed in the near-threshold region by the present calculation. The probable reason for this is easy to understand. The cross section near threshold is dominated by the ${}^2B_{2g}$ symmetry of the elastic-channel shape resonance, and the sharp threshold rise of the excitation cross section is due to the tail of that resonance. When polarization effects are included, the resonance moves down in energy, the triplet threshold thus lies farther out in the tail of the resonance, and the ${}^2B_{2g}$ contribution to the excitation cross section decreases dramatically. These results thus illustrate the important effect that polarization can have on electronic excitation cross sections, as recently emphasized by da Costa *et al.* [12,35].

The present work extends the measurements of the elastic cross sections to larger scattering angles and to lower energies. Very good agreement is found with recent calculations which take into account target polarization.

ACKNOWLEDGMENTS

We thank Cynthia Trevisan and Tom Rescigno for providing their calculated cross sections in numerical form and

Marco A. P. Lima for helpful discussions. This research is part of Swiss National Science Foundation Project No. 200020-113599/1. The work of C.W. and V.M. was supported by the Chemical Sciences, Geosciences, and Bio-

sciences Division, Office of Basic Energy Sciences, Office of Science, U.S. Department of Energy, and employed the resources of the Jet Propulsion Laboratory's Supercomputing and Visualization Facility.

-
- [1] O. Sueoka and S. Mori, *J. Phys. B* **19**, 4035 (1986).
[2] B. Mapstone and W. R. Newell, *J. Phys. B* **25**, 491 (1992).
[3] S. L. Lunt, J. Randell, J. P. Ziesel, G. Mrotzek, and D. Field, *J. Phys. B* **27**, 1407 (1994).
[4] R. Panajotovic, M. Kitajima, H. Tanaka, M. Jelisavcic, J. Lower, L. Campbell, M. J. Brunger, and S. J. Buckman, *J. Phys. B* **36**, 1615 (2003).
[5] M. A. Khakoo, K. Keane, C. Campbell, N. Guzman, and K. Hazlett, *J. Phys. B* **40**, 3601 (2007).
[6] C. Winstead, P. Hipes, M. A. P. Lima, and V. McKoy, *J. Chem. Phys.* **94**, 5455 (1991).
[7] C. Winstead, V. McKoy, and M. H. F. Bettega, *Phys. Rev. A* **72**, 042721 (2005).
[8] B. I. Schneider, T. N. Rescigno, B. H. Lengsfeld, and C. W. McCurdy, *Phys. Rev. Lett.* **66**, 2728 (1991).
[9] C. S. Trevisan, A. E. Orel, and T. N. Rescigno, *Phys. Rev. A* **68**, 062707 (2003).
[10] Q. Sun, C. Winstead, V. McKoy, and M. A. P. Lima, *J. Chem. Phys.* **96**, 3531 (1992).
[11] T. N. Rescigno and B. I. Schneider, *Phys. Rev. A* **45**, 2894 (1992).
[12] R. F. da Costa, M. H. F. Bettega, L. G. Ferreira, and M. A. P. Lima, *J. Phys.: Conf. Ser.* **88**, 012028 (2007).
[13] E. H. Van Veen, *Chem. Phys. Lett.* **41**, 540 (1976).
[14] D. E. Love and K. D. Jordan, *Chem. Phys. Lett.* **235**, 479 (1995).
[15] M. Allan, *Chem. Phys. Lett.* **225**, 156 (1994).
[16] K. R. Asmis and M. Allan, *J. Chem. Phys.* **106**, 7044 (1997).
[17] M. Allan, *J. Phys. B* **38**, 3655 (2005).
[18] F. H. Read and J. M. Channing, *Rev. Sci. Instrum.* **67**, 2372 (1996).
[19] M. Allan, *J. Phys. B* **25**, 1559 (1992).
[20] M. Allan, *J. Phys. B* **40**, 3531 (2007).
[21] A. Gopalan, J. Bömmels, S. Götte, A. Landwehr, K. Franz, M. W. Ruf, H. Hotop, and K. Bartschat, *Eur. Phys. J. D* **22**, 17 (2003).
[22] J. C. Nickel, P. W. Zetner, G. Shen, and S. Trajmar, *J. Phys. E* **22**, 730 (1989).
[23] R. K. Nesbet, *Phys. Rev. A* **20**, 58 (1979).
[24] M. Zubek, N. Gulley, G. C. King, and F. H. Read, *J. Phys. B* **29**, L239 (1996).
[25] K. Takatsuka and V. McKoy, *Phys. Rev. A* **24**, 2473 (1981); **30**, 1734 (1984).
[26] C. Winstead and V. McKoy, *Adv. At., Mol., Opt. Phys.* **36**, 183 (1996).
[27] C. Winstead and V. McKoy, *Comput. Phys. Commun.* **128**, 386 (2000).
[28] C. W. Bauschlicher, *J. Chem. Phys.* **72**, 880 (1980).
[29] W. J. Hunt and W. A. Goddard III, *Chem. Phys. Lett.* **3**, 414 (1969).
[30] M. Hayashi, in *Non-Equilibrium Processes in Partially Ionized Gases*, edited by M. Capitelli and J. N. Bardsley (Plenum, New York, 1990), p. 333.
[31] M. Allan, in *Atomic and Molecular Data and Their Applications*, edited by E. Roueff, AIP Conf. Proc. No. 901 (AIP, Melville, NY, 2007), p. 107.
[32] I. C. Walker, A. Stamatovic, and S. F. Wong, *J. Chem. Phys.* **69**, 5532 (1978).
[33] K. D. Jordan and P. D. Burrow, *Chem. Rev. (Washington, D.C.)* **87**, 557 (1987).
[34] M. Allan, *J. Electron Spectrosc. Relat. Phenom.* **48**, 219 (1989).
[35] R. F. da Costa, M. H. F. Bettega, and M. A. P. Lima, *Phys. Rev. A* **77**, 012717 (2008).